Spin-orbit-stable type-II nodal line band crossing in *n*-doped monolayer MoX_2 (X = S, Se,Te)

Kyung-Han Kim,[1] Bohm Jung Yang,[2,3,4] and Hyun-Woo Lee[1,*]

[1]*Department of Physics, Pohang University of Science and Technology, Pohang 37673, Korea*
[2]*Department of Physics and Astronomy, Seoul National University, Seoul 08826, Korea*
[3]*Center for Correlated Electron Systems, Institute for Basic Science (IBS), Seoul 08826, Korea*
[4]*Center for Theoretical Physics (CTP), Seoul National University, Seoul 08826, Korea*

(Received 24 August 2018; published 26 December 2018)

1H-phase monolayer transition-metal dichalcogenides have spin-split electronic band structures near the $K(K')$ point due to strong spin-orbit coupling and intrinsic inversion symmetry breaking. In the case of the monolayer MoX_2 (X = S, Se, Te), the spin-split conduction bands cross near the $K(K')$ point. We show that the band crossing occurs not only along the high-symmetry directions, but also along arbitrary directions due to a mirror reflection symmetry of the monolayer. As a result, n-doped monolayer MoX_2 is a two-dimensional type-II nodal-line material.

DOI: 10.1103/PhysRevB.98.245422

I. INTRODUCTION

Dirac and Weyl semimetals have been extensively investigated due to their unique topological properties [1]. Recently, nodal line semimetal has also attracted huge attention as a kind of topological semimetal [2]. So far, several materials are proposed as a three-dimensional (3D) nodal line semimetal such as 3D graphene, Cu_3PdN, AX_2 (A = Ca, Sr, Ba; X = Si, Ge, Sn), CaTe, Mg_3Bi_2, β-PbO_2, and CaP_3 family of materials [3–9]. These proposals are however based on the assumption that there is no spin-orbit coupling (SOC). When SOC is taken into account, the nodal line structure in the materials is broken, though weakly since SOC is weak. A recent first-principles calculation [10] combined with an effective model analysis predicts that layered ferromagnetic rare-earth-metal monohalides are 3D nodal line semimetal with SOC. Until now, $PbTaSe_2$ is the only material that is confirmed experimentally as a 3D nodal line semimetal with strong SOC [11].

The concepts of Dirac, Weyl, and nodal lines are applicable to two dimensions as well. Several theoretical calculations [12–14] predicted nodal line band crossing in 2D materials with weak SOC. But similarly to the 3D case, the nodal line band crossing in the materials is broken when SOC is taken into account. An experiment [15] reported the realization of 2D Dirac nodal line fermions in monolayer Cu_2Si with weak SOC. When SOC is taken into account theoretically, however, the nodal line band crossing in this material is also broken. A recent theory [16] classifies all possible band crossing structures in time-reversal invariant 2D noncentrosymmetric systems *with SOC*. According to the theory, the nodal line crossing can be stable with respect to SOC if materials have proper geometrical symmetries. Weak SOC materials (Be_2C, BeH_2) [17] and Na_2CrBi trilayer [18] are theoretically proposed as type-I 2D nodal line materials with SOC.

In this paper, we report that n-doped monolayer MoX_2 (X = S, Se, Te) (Fig. 1), which is a well-known monolayer transition-metal dichalcogenide (TMD) material, has a type-II nodal line band crossing that remains robust even though the monolayer has strong SOC. This example of the 2D type-II nodal line material has strong SOC. The nodal line band crossing is demonstrated by combining tight-binding model calculation with symmetry analysis. It has been already known [20–26] that the lowest conduction band of the monolayer MoX_2 has band crossing near the $K(K')$ point along the $\Gamma - K(K')$ line. The main point of this paper is that the band crossing appears not only along the high-symmetry directions, but also along arbitrary directions, thereby forming a nodal line band crossing near the $K(K')$ point.

II. THEORY

In this section, we demonstrate that the 1H phase monolayer MoX_2 has the nodal line band crossing and that the crossing remains stable despite SOC due to its $\hat{M}_z$ mirror reflection symmetry [Fig. 1(a)]. We use the tight-binding Hamiltonian of the 1H phase monolayer MoS_2 [21] to calculate the energy band structure, which is shown along the Γ-K line in Fig. 2(a). As illustrated in Fig. 2, the spin-up conduction band and the spin-down conduction band cross near the K point and forms a type-II nodal line band crossing.

To check if the structure in Fig. 2(b) is a true nodal line crossing structure or an anticrossing structure with small energy separation, we utilize a recent theoretical result [16], which classifies band crossings and emergent semimetals in two-dimensional noncentrosymmetric systems. According to the classification, nodal line semimetal phase is topologically stable in 2D material if (i) there exists mirror reflection symmetry about the material's 2D plane and (ii) the two bands which are crossing each other have different mirror eigenvalues.

In the case of the 1H phase monolayer MoX_2, it is invariant under the mirror reflection about the xy plane (Fig. 1),

*hwl@postech.ac.kr

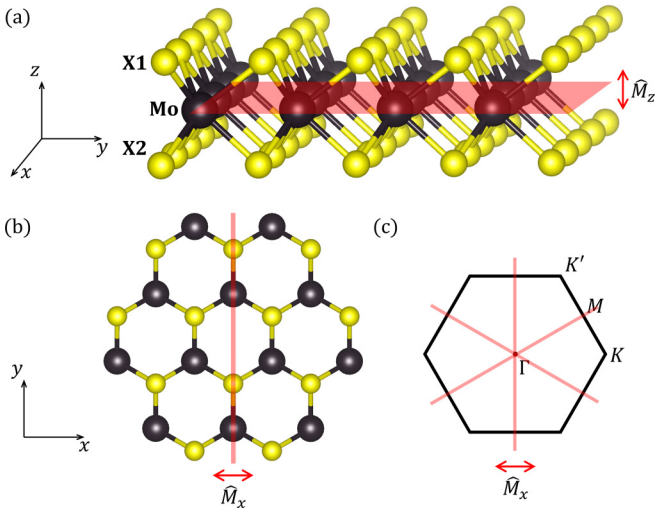

FIG. 1. (a) Side view and (b) top view of a $1H$ phase monolayer MoX_2 [19], which consists of Mo atoms (larger dot) and X atoms (smaller dot). It has mirror reflection symmetry with respect to the middle sublayer plane ($\hat{M}_z$) and the perpendicular bisector plane ($\hat{M}_x$). (c) First Brillouin zone in the momentum space with $\hat{M}_x$ mirror symmetry invariant line (red).

so the condition (i) is satisfied. Then the Hamiltonian H of the monolayer should commute with the mirror reflection operator $\hat{M}_z$,

$$[H, \hat{M}_z] = 0. \tag{1}$$

Since $\hat{M}_z$ does not modify the 2D crystal momentum $\mathbf{k}$, this commutation relation implies that energy eigenstates with the crystal momentum $\mathbf{k}$ are eigenstates of $\hat{M}_z$. Since the eigenvalue spectrum of $\hat{M}_z$ is discrete, the continuous variation of

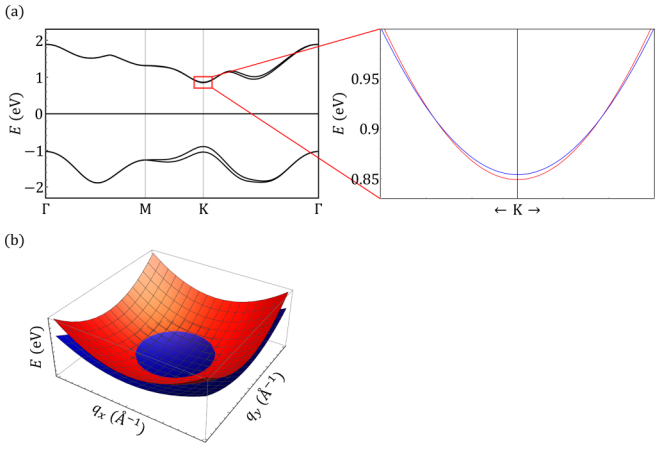

FIG. 2. (a) Tight-binding band structure of conduction and valence bands of the $1H$ phase monolayer MoS_2 with the SOC. In the rectangular region near the K point, there is band crossing of the conduction bands which makes a nodal line band structure. Here the colors indicate states with the out-of-plane spin up (red) and down (blue), respectively. (b) Schematic 3D plot of the conduction bands near the K point ($\boldsymbol{q} = \boldsymbol{k} - \boldsymbol{K} = 0$). It shows the nodal line band crossing between the spin-up and -down bands. Trigonal warping effect is too weak to be seen near the conduction-band minimum.

energy eigenstates as a function of $\mathbf{k}$ within an energy band cannot alter the eigenvalue of $\hat{M}_z$ (or mirror eigenvalue). Thus one finds that each energy band of H has a well defined mirror eigenvalue.

Now, we consider the mirror eigenvalues of the two conduction bands depicted in Fig. 2. To check if the two conduction bands satisfy the conduction (ii), crude information on the wave-function character of the two conduction bands is sufficient since possible mirror eigenvalues are discrete and the mirror eigenvalue of each band can be determined from crude wave-function characters. In this regard, the wave-function character near the K point is sufficient. The K point has the C_{3h} point-group symmetry. Using its irreducible representations [27], the wave functions of the two conduction bands at the K point can be expressed as

$$\left[\alpha^{\mathrm{Mo}}\left|\Psi^{\mathrm{Mo}}_{2,0}\right\rangle + \frac{\alpha^{\mathrm{X}}}{\sqrt{2}}\left(\left|\Psi^{\mathrm{X1}}_{1,1}\right\rangle + \left|\Psi^{\mathrm{X2}}_{1,1}\right\rangle\right)\right] \otimes |\chi\rangle, \tag{2}$$

where χ is spin-up or -down states, α is the ratio of each orbital wave function, and the superscript indicates at which atom the corresponding wave function is localized. $X1$ and $X2$ in the superscript denotes upper and lower X atoms. The subscript denotes, on the other hand, spherical harmonics information of the wave function. From the character table of the group C_{3h} [27], or just considering the spherical harmonics information in the orbital part wave-function character of the conduction bands in Eq. (2), one finds that the orbital part wave functions of the two conduction bands are even about $\hat{M}_z$. Since wave functions consist of orbital and spin parts, one needs to figure out the effect of $\hat{M}_z$ on the spin part wave function as well. For this, we utilize the relation $\hat{M}_z = \hat{I}\exp[-i(L_z + S_z)\pi/\hbar]$, where $\hat{I}$ denotes the inversion operator, and L_z (S_z) denotes the orbital (spin) angular momentum operator along the out-of-plane direction. Thus one obtains $\hat{M}_z|\uparrow\rangle = -i|\uparrow\rangle$ and $\hat{M}_z|\downarrow\rangle = +i|\downarrow\rangle$. Then one finds

$$\hat{M}_z|\psi_{\mathrm{cb}}(\boldsymbol{r})\rangle \otimes |\uparrow\rangle = -i|\psi_{\mathrm{cb}}(\boldsymbol{r})\rangle \otimes |\uparrow\rangle, \tag{3}$$

$$\hat{M}_z|\psi_{\mathrm{cb}}(\boldsymbol{r})\rangle \otimes |\downarrow\rangle = i|\psi_{\mathrm{cb}}(\boldsymbol{r})\rangle \otimes |\downarrow\rangle. \tag{4}$$

Since the two conduction bands share the same orbital character but have opposite spin character, this means that the spin-up and spin-down conduction bands have different mirror eigenvalues ($-i$ and $+i$, respectively). Therefore the two conduction bands satisfy the condition (ii) as well near the K point. This verifies that there exists band crossing along arbitrary directions near the K point and the resulting nodal line band crossing near the K point is stable topologically. An exactly same kind of analysis applies to the type-II nodal line structure band crossing near the K' point as well since the wave function characters of the conduction-band energy eigenstates at the K' point is obtained by complex conjugation of the corresponding wave function characters at the K point.

III. DISCUSSION

In the previous section, we showed that if the spin split bands are ordered as Fig. 2 to form band crossing near the $K(K')$ point, there should appear a true nodal line structure that is stable against anticrossing since the anticrossing is

forbidden by the $\hat{M}_z$ mirror symmetry. According to first-principles calculations [22–26], the band splitting between the two conduction bands near the K and K' points are negative (meaning band crossing) for MoX_2 (-3 meV for MoS_2, -22 meV for $MoSe_2$, -36 meV for $MoTe_2$) and positive (meaning no band crossing) for WX_2 (32 meV for WS_2, 37 meV for WSe_2, 52 meV for WTe_2). In the case of $MoSe_2$ (WS_2, WSe_2), optical experiments [26,28–32] also support the band crossing (no crossing). Based on these results, we then conclude that there should appear a type-II nodal line structure in MoX_2. One cautionary remark is in order. In the case of MoS_2, the band splitting is very small and thus further studies are necessary to confirm the predicted band structure. The reason why the conduction-band spin split ordering is different between MoX_2 and WX_2 is that the level spacing between the two conduction bands with opposite spin is affected in different ways in Mo-based and W-based TMD materials by the competition between the first-order SOC contribution from the chalcogen atom's orbitals and the second-order SOC contribution from the transition metal's orbitals [20,24].

According to DFT calculation of $1H$ phase monolayer MoS_2 [24], the nodal line band crossing occurs about 50 meV above the conduction-band minimum and the **k**-space area enclosed by the nodal line occupies about 1.5% of the first Brillouin zone. In this respect, it is worth noting that even without any intentional doping, monolayer MoS_2 is naturally doped [33] due to the interaction between the MoS_2 monolayer and its substrate. Many experiments find this natural doping to be n type for typical dielectric substrates [34]. Thus it is plausible that mild additional n doping of the monolayer MoS_2 can bring the Fermi energy close to the nodal line crossing. When such Fermi energy tuning is achieved, this kind of nodal line band crossing has the potential to show interesting physics. For instance, it is predicted [35–37] that large Berry curvature is generated when the nodal line band crossing is gapped out by the symmetry breaking. By the way, we remark that the type-II nodal line band crossing does not make n-doped monolayer MoS_2 a semimetal, since the crossing does not suppress the density of states in 2D materials.

Now we consider the stability of the nodal line band crossing against the symmetry breaking. When the $\hat{C}_3$ rotational symmetry is broken, the nodal line is still stable due to the $\hat{M}_z$ mirror symmetry. However, when the $\hat{M}_z$ mirror symmetry is broken, the nodal line is no longer stable, and may evolve to either type-II Dirac points or anticrossing structure. The type-II nodal line structure evolves to type-II Dirac points if some points on the nodal line remain degenerate due to remaining symmetries after the $\hat{M}_z$ mirror symmetry breaking. In this case, MoX_2 has the $\hat{M}_x$ mirror symmetry and this symmetry can guarantee such degeneracy on the $\hat{M}_x$ mirror invariant line. However as shown in Figs. 1(b) and 1(c), the $K(K')$ point is not on the $\hat{M}_x$ mirror symmetry line which is along the ΓM line in the momentum space, so the nodal line band crossing becomes an anticrossing band structure.

In summary, we showed that the $1H$ phase monolayer MoX_2 has nodal line band crossing near the $K(K')$ point and this band crossing is protected along the arbitrary directions by mirror reflection symmetry about a 2D plane. As a result, n-doped monolayer MoX_2 is predicted to be a type-II nodal line material with strong SOC.

ACKNOWLEDGMENTS

We acknowledge fruitful discussion with Y. Kim. K.H.K. and H.W.L. were supported by the National Research Foundation of Korea (Grant No. 2018R1A5A6075964). B.-J.Y. was supported by the Institute for Basic Science in Korea (Grant No. IBS-R009-D1), Basic Science Research Program through the National Research Foundation of Korea (NRF) (Grants No. 0426-20170012 and No. 0426-20180011), the POSCO Science Fellowship of POSCO TJ Park Foundation (Grant No. 0426-20180002), U.S. Army Research Office under Grant No. W911NF-18-1-0137.

[1] N. P. Armitage, E. J. Mele, and A. Vishwanath, Rev. Mod. Phys. **90**, 015001 (2018).
[2] S. Yang, H. Yang, E. Derunova, S. S. P. Parkin, B. Yan, and M. N. Ali, Adv. Phys.: X **3**, 1414631 (2018).
[3] H. Weng, Y. Liang, Q. Xu, R. Yu, Z. Fang, X. Dai, and Y. Kawazoe, Phys. Rev. B **92**, 045108 (2015).
[4] R. Yu, H. Weng, Z. Fang, X. Dai, and X. Hu, Phys. Rev. Lett. **115**, 036807 (2015).
[5] H. Huang, J. Liu, D. Vanderbilt, and W. Duan, Phys. Rev. B **93**, 201114(R) (2016).
[6] Y. Du, F. Tang, D. Wang, L. Sheng, E. Kan, C. Duan, S. Y. Savrasov, and X. Wan, npj Quantum Mater. **2**, 3 (2017).
[7] X. Zhang, L. Jin, X. Dai, and G. Liu, J. Phys. Chem. Lett. **8**, 4814 (2017).
[8] Z. Wang and G. Wang, Phys. Lett. A **381**, 2856 (2017).
[9] Q. Xu, R. Yu, Z. Fang, X. Dai, and H. Weng, Phys. Rev. B **95**, 045136 (2017).
[10] S. Nie, H. Weng, and F. B. Prinz, arXiv:1803.08486.
[11] G. Bian, T. Chang, R. Sankar, S. Xu, H. Zheng, T. Neupert, C. Chiu, S. Huang, G. Chang, I. Belopolski, D. S. Sanchez, M. Neupane, N. Alidoust, C. Liu, B. Wang, C. Lee, H. Jeng, C. Zhang, Z. Yuan, S. Jia *et al.*, Nat. Commun. **7**, 10556 (2016).
[12] J.-L. Lu, W. Luo, X.-Y. Li, S.-Q. Yang, J.-X. Cao, X.-G. Gong, and H.-J. Xiang, Chin. Phys. Lett. **34**, 057302 (2017).
[13] Y.-J. Jin, R. Wang, J.-Z. Zhao, Y.-P. Du, C.-D. Zheng, L.-Y. Gan, J.-F. Liu, H. Xu, and S. Y. Tong, Nanoscale **9**, 13112 (2017).
[14] P. Zhou, Z. S. Ma, and L. Z. Sun, J. Mater. Chem. C **6**, 1206 (2018).
[15] B. Feng, B. Fu, S. Kasamatsu, S. Ito, P. Cheng, C. Liu, Y. Feng, S. Wu, S. K. Mahatha, P. Sheverdyaeva, P. Moras, M. Arita, O. Sugino, T. Chiang, K. Shimada, K. Miyamoto, T. Okuda, K. Wu, L. Chen, Y. Yao, and I. Matsuda, Nat. Commun. **8**, 1007 (2017).
[16] S. Park and B.-J. Yang, Phys. Rev. B **96**, 125127 (2017).
[17] B. Yang, X. Zhang, and M. Zhao, Nanoscale **9**, 8740 (2017).
[18] C. Niu, P. M. Buh, H. Zhang, G. Bihlmayer, D. Wortmann, S. Blügel, and Y. Mokrousov, arXiv:1703.05540.

[19] K. Momma and F. Izumi, J. Appl. Crystallogr. **44**, 1272 (2011).
[20] G.-B. Liu, W.-Y. Shan, Y. Yao, W. Yao, and D. Xiao, Phys. Rev. B **88**, 085433 (2013).
[21] H. Rostami, R. Roldán, E. Cappelluti, R. Asgari, and F. Guinea, Phys. Rev. B **92**, 195402 (2015).
[22] K. Kośmider, J. W. González, and J. Fernández-Rossier, Phys. Rev. B **88**, 245436 (2013).
[23] A. Kormányos, V. Zólyomi, N. D. Drummond, and G. Burkard, Phys. Rev. X **4**, 011034 (2014).
[24] A. Kormányos, G. Burkard, M. Gmitra, J. Fabian, V. Zólyomi, N. D. Drummond, and V. I. Fal'ko, 2D Mater. **2**, 022001 (2015).
[25] J. P. Echeverry, B. Urbaszek, T. Amand, X. Marie, and I. C. Gerber, Phys. Rev. B **93**, 121107(R) (2016).
[26] M. Koperski, M. R. Molas, A. Arora, K. Nogajewski, A. O. Slobodeniuk, C. Faugeras, and M. Potemski, Nanophotonics **6**, 1289 (2017).
[27] A. Kormányos, V. Zólyomi, N. D. Drummond, P. Rakyta, G. Burkard, and V. I. Fal'ko, Phys. Rev. B **88**, 045416 (2013).
[28] Z. Ye, T. Cao, K. O'Brien, H. Zhu, X. Yin, Y. Wang, S. G. Louie, and X. Zhang, Nature (London) **513**, 214 (2014).
[29] A. Arora, K. Nogajewski, M. Molas, M. Koperski, and M. Potemski, Nanoscale **7**, 20769 (2015).
[30] G. Wang, C. Robert, A. Suslu, B. Chen, S. Yang, S. Alamdari, I. C. Gerber, T. Amand, X. Marie, S. Tongay, and B. Urbaszek, Nat. Commun. **6**, 10110 (2015).
[31] M. R. Molas, C. Faugeras, A. O. Slobodeniuk, K. Nogajewski, M. Bartos, D. M. Basko, and M. Potemski, 2D Mater. **4**, 021003 (2017).
[32] X.-X. Zhang, T. Cao, Z. Lu, Y.-C. Lin, F. Zhang, Y. Wang, Z. Li, J. C. Hone, J. A. Robinson, D. Smirnov, S. G. Louie, and T. F. Heinz, Nat. Nanotechnol. **12**, 883 (2017).
[33] K. Dolui, I. Rungger, and S. Sanvito, Phys. Rev. B **87**, 165402 (2013).
[34] D. Sercombe, S. Schwarz, O. D. Pozo-Zamudio, F. Liu, B. J. Robinson, E. A. Chekhovich, I. I. Tartakovskii, O. Kolosov, and A. I. Tartakovskii, Sci. Rep. **3**, 3489 (2013).
[35] K. H. Kim and H. W. Lee, Phys. Rev. B **97**, 235423 (2018).
[36] B. T. Zhou, K. Taguchi, Y. Kawaguchi, Y. Tanaka, and K. T. Law, arXiv:1712.02942.
[37] A. S. Patri, K. Hwang, H. Lee, and Y. B. Kim, Sci. Rep. **8**, 8052 (2018).